JOURNAL OF APPLIED ELECTROCHEMISTRY 17 (1987) 1304–1314

# *Choked two-phase flow during electrochemical machining*

I. ROUŠAR

*Department of Inorganic Technology, Institute of Chemical Technology, 166 28 Prague 6, Czechoslovakia*

Received 19 January 1987; revised 9 June 1987

A one-dimensional, two-phase fluid flow theory is formulated for the electrolyte–gas mixture behaviour in the interelectrode gap during electrochemical machining. The condition for generating the choked two-phase flow is described by an analytical formula. The initiation of choked two-phase flow in a flat, axially symmetric cavity is discussed.

**Nomenclature**

| | |
|---|---|
| $A(s)$ | total area (cross-section of interelectrode gap ($m^2$) |
| $A_g$, $A_f$ | cross-section of interelectrode gap filled with gas and electrolyte, respectively ($m^2$) |
| $c_p$ | specific heat of electrolyte ($J\,kg^{-1}\,K^{-1}$) |
| $d$ | diameter of inlet tube for flat radial cathode (tool (m) |
| $d_g$, $d_f$, $d_m$ | densities of gas, electrolyte and anode metal, respectively ($kg\,m^{-3}$) |
| $d_R$ | density ratio (see Equation 28) |
| $D$ | outer diameter of flat tool (m) |
| $E$ | voltage drop in interelectrode gap (V) |
| $E_A$, $E_C$ | potentials of anode and cathode (V) |
| $Eu$ | Euler number (see Equation 29) |
| $f$ | multiplier of $dp/ds$ (see Equation 27) |
| $f_r$ | tool feed rate ($m\,s^{-1}$) |
| $F$ | Faraday constant, 96487 ($A\,s\,mol^{-1}$) |
| $g(s)$ | thickness of interelectrode gap (m) |
| $g_0$, $g_e$ | inlet and outlet (exit) values of $g(s)$ (m) |
| $h_a$, $h_f$ | enthalpies of anode metal and electrolyte, respectively ($J\,kg^{-1}$) |
| $L$ | length of gap (m) |
| $m_a$ | mass flux rate for anode dissolution ($kg\,m^{-2}\,s^{-1}$) |
| $M_{g,c}$ | molar mass of hydrogen or inert gas present in electrolyte ($kg\,mol^{-1}$) |
| $i$ | current density ($A\,cm^{-2}$) |
| $I$ | total current (A) |
| $p(s)$ | static pressure in interelectrode gap (Pa) |
| $p_0$, $p_e$ | static pressures at inlet and outlet of the gap, respectively (Pa) |
| $P(s)$ | perimeter of the tool at distance $s$ (m) |
| $R_g$ | gas constant, 8.31471 $J\,mol^{-1}\,K^{-1}$ |
| $Re_M$ | Reynolds number (see Equation 23) |
| $s$ | coordinate along gap (m) |
| $T(s)$ | electrolyte temperature in interelectrode gap (K) |
| $T_0$, $T_e$ | temperatures at inlet and outlet parts of gap (K) |
| $v_g$, $v_f$ | linear velocities of gas and electrolyte, respectively ($m\,s^{-1}$) |
| $V_a$ | velocity of anode dissolution ($m\,s^{-1}$) |
| $V_c$ | velocity of tool (cathode) ($m\,s^{-1}$) |
| $\dot{V}_g$, $\dot{V}_f$ | volume flow rates of gas and electrolyte, respectively ($m^3\,s^{-1}$) |
| $y_g$, $y_f$ | part of the interelectrode gap filled with gas or electrolyte, respectively (m) |
| $\alpha_M$ | limiting volume fraction of gas in electrolyte, calculated as right-hand side of Equation 30c |
| $\alpha(s)$ | volume fraction of gas in electrolyte |
| $\alpha_0$, $\alpha_e$ | volume fractions of gas at inlet and outlet, respectively |
| $\gamma_R$ | temperature coefficient of specific resistivity, see Equation 12 ($K^{-1}$) |



0021–891X/87 $03.00 + .12 

| | | | |
|---|---|---|---|
| $\varepsilon_a$, $\varepsilon_c$ | electrochemical equivalents for dissolution of anode material and for gas evolution on cathode ($kg\,C^{-1}$) | $\varrho_M$ | specific resistivity of gas–electrolyte mixture ($\Omega m$) |
| | | $\varrho_{f,0}$ | specific resistivity of electrolyte at inlet ($\Omega m$) |
| $\Theta$ | angle (see Fig. 1) | $\sigma$ | slip ratio (for bubbles in the electrolyte) |
| $\nu_f$ | kinematic viscosity of electrolyte ($m^2\,s^{-1}$) | | |

## 1. Introduction

The electrochemical machining of metals involves the anodic dissolution of metals at current densities 5–350 $A\,cm^{-2}$ using a cathode of given surface geometry. The interelectrode gap is usually very small (0.05–1.3 mm) and the linear velocity of the electrolyte in the interelectrode gap is 3–20 $m\,s^{-1}$. Due to gas evolution on the cathode and heat generation in the electrolyte the conditions along the flow path are changing and thus lead to a non-uniform current density distribution over the anode surface [1–3]. A more uniform current density distribution can be obtained by using a mixture of air and electrolyte ($\sim 1:1$) (at inlet pressure up to 1.6 MPa) and a flow restrictor dam at the exit [4]. Nevertheless, this increases the possibility of choking in the interelectrode gap. Choking was discussed for shallow axially symmetric cavities by Thorpe and Zerkle [5]. An evaluation of the true conditions for choking is the subject of this study.

## 2. Theory

The choking condition for the two-phase flow is fulfilled if the static pressure in the interelectrode gap increases to infinity. Instability occurs in the flow regime and these instabilities are well developed in the case of axially symmetric cavities (gaps). This is why we introduce here a system with axial symmetry, but the results are also valid for flat ducts and other systems where the approximation of plug flow is reasonable. The system with axial symmetry is shown in Fig. 1.

The flow in the interelectrode gap is assumed to be one-dimensional, with only one independent space variable, $s$, along the gap ($s = 0$ for $r = d/2$). The flow of electrolyte (mixed with inert gas) is radially outward in a thin gap, $g(s)$. The length of the gap $L \gg g(s)$. The tool (cathode) moves down at the feed rate, $f_r$. The normal velocity of the cathode, $V_c$, depends on position s.

$$V_c = f_r \cos \Theta(s) \tag{1}$$

At the anode the current flux dissolves the anode material and the anode surface moves down at velocity $V_a$. The dissolved materials enters the electrolyte and flows out as sludge. Since the content of sludge in the electrolyte is small, the properties of the electrolyte are assumed to be independent of sludge content.

It is assumed that the gap can be formally lumped to equivalent heights: $y_f$ (filled with electrolyte) and $y_g$ (filled with gas).

Then

$$g(s) = y_g(s) + y_f(s) \tag{2}$$

and the void fraction, $\alpha$, is defined as

$$\alpha = \frac{y_g(s)}{g(s)} \tag{3a}$$

$$1 - \alpha = \frac{y_f(s)}{g(s)} \tag{3b}$$

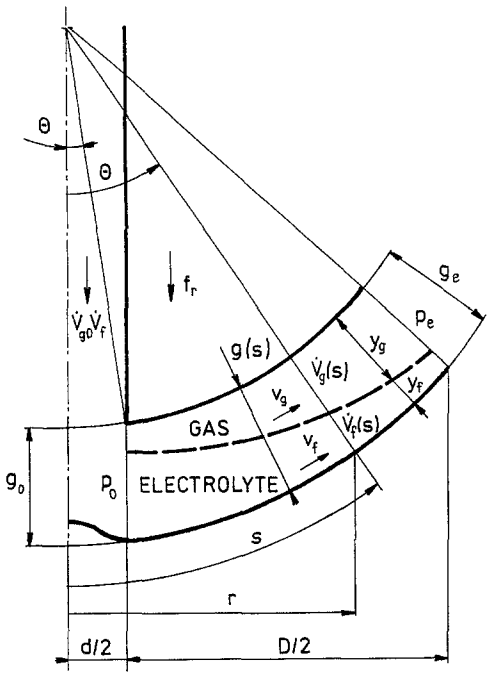


Fig. 1. Schematic representation of ECM system with axial symmetry. $\dot{V}_{g,o}$, Volumetric flow rate of inert gas at inlet; $f_r$, feed rate of cathode; $r$, radius (see Nomenclature for other symbols).

The value of $v_g$ is assumed to be equal to $v_f$. Then $\sigma$ is equal to one, i.e.

$$\sigma = \frac{v_g}{v_f} = 1 \tag{4}$$

The void fraction can be expressed from $A_g$ and $A_f$,

$$A_g = 2\pi r(s) y_g(s) \tag{5a}$$

$$A_f = 2\pi r(s)\, y_f(s) \tag{5b}$$

giving

$$\alpha = \frac{A_g}{A_g + A_f} \tag{6a}$$

or by $\dot{V}_g$ and $\dot{V}_f$, giving

$$\alpha = \frac{\dot{V}_g}{\dot{V}_g + \dot{V}_f} \tag{6b}$$

The time dependence of the gap thickness is given by $V_c$ and $V_a$,

$$\frac{\partial g}{\partial \tau} = V_a - V_c \tag{7}$$

and $V_a$ is given by Equation 8 and $V_c$ by Equation 1

$$V_a = \frac{m_a}{d_m} \tag{8}$$

where $m_a$ can be expressed using $\varepsilon_A$

$$m_a = \varepsilon_a i \tag{9a}$$

Obviously, for the gas mass flux it holds that

$$m_g = \varepsilon_c i \tag{9b}$$

Combining Equations 1, 7, 8 and 9 we obtain

$$\frac{\partial g}{\mathrm{d}t} = \frac{\varepsilon_a i}{d_m} - f_r \cos \Theta \tag{10a}$$

and for the steady state ($\partial g/\partial \tau = 0$) we have

$$i = \frac{d_m}{\varepsilon_A} f_r \cos \Theta \tag{10b}$$

The current density may be calculated for each current line from the relation

$$U = ig(s)\, \varrho_M(s) + E_A(i) - E_C(i) \tag{11}$$

Where the first term on the right hand side represents the voltage drop in the interelectrode gap $g(s)$. The specific resistivity of the mixture of bubbles and electrolyte is given by the Bruggeman equation:

$$\varrho_M(s) = \varrho_{f0}[1 + \gamma_R(T(s) - T_0)]\left[1 + \frac{\dot{V}_g(s)}{\dot{V}_f(s)}\right]^{1.5} \tag{12}$$

where $\gamma_R = (\partial \ln \varrho_f/\partial T)$.

Following Thorpe and Zerkle [5] it is assumed that the dependence of the electrode potentials on the local current density can be neglected. Further, it is assumed that the voltage drop in the electrolyte has a constant value, $E$, independent of the time and space coordinate, $s$:

$$E = U - E_A + E_C = \text{constant} \tag{13}$$

The equation of continuity for the gas phase is

$$\frac{\partial(d_g A_g)}{\partial \tau} = P(s)\, m_g - \frac{\partial(d_g \dot{V}_g)}{\partial s} \tag{14a}$$

where $P(s)$ is the tool perimeter ($= 2\pi r(s)$) at the distance $s$.

For the steady state ($\partial(d_g A_g)/\partial \tau = 0$) and using Equation 9b,

$$\frac{\mathrm{d}(d_g \dot{V}_g)}{\mathrm{d}s} = 2\pi r(s) \varepsilon_c i \tag{14b}$$

For the calculation of $d_g$ the equation of state for an ideal gas can be used, giving

$$d_g = M_{g,c}\left(\frac{p}{R_g T}\right) \tag{15}$$

From Equations 14b and 15,

$$\frac{\mathrm{d}\dot{V}_g}{\mathrm{d}s} = \frac{R_g T}{M_{g,c} p} 2\pi r(s) \varepsilon_c i - \left(\frac{\dot{V}_g}{p}\right)\left(\frac{\mathrm{d}p}{\mathrm{d}s}\right) + \left(\frac{\dot{V}_g}{T}\right)\left(\frac{\mathrm{d}T}{\mathrm{d}s}\right) \tag{16}$$

The equation of continuity for the fluid flow is

$$\frac{\partial(d_f A_f)}{\partial \tau} = -\frac{\partial(d_f \dot{V}_f)}{\partial s} + [2\pi r(s)]\,(m_a - m_g) \tag{17a}$$

and for the steady state ($\partial(d_f \dot{V}_f)/\partial \tau = 0$), using the assumption that $d_f \neq f(T, s)$ and Equations 9a

and 9b, it follows that

$$\frac{\mathrm{d}\dot{V}_\mathrm{f}}{\mathrm{d}s} = \frac{[2\pi r(s)\, i(s)]\,(\varepsilon_\mathrm{A} - \varepsilon_\mathrm{C})}{d_\mathrm{f}} \tag{17b}$$

The transport of energy is due mainly to the electrolyte flow; the transport of energy by gas is assumed negligible compared to that by electrolyte. The transfer of heat from the electrolyte to the metal is also neglected. This implies an adiabatic process with Joule heat generated in th eelectrolyte according to

$$\left(\frac{\partial}{\partial\tau}\right)(d_\mathrm{f}A_\mathrm{f}u_\mathrm{f}) = -\left(\frac{\partial}{\partial s}\right)(d_\mathrm{f}\dot{V}_\mathrm{f}h_\mathrm{f}) + 2\pi r(s)\, i(s)E \tag{18}$$

where $u_\mathrm{f}$ and $h_\mathrm{f}$ are the internal energy and the specific enthalpy of the electrolyte, respectively.

For the steady state $\partial(d_\mathrm{f}\, A_\mathrm{f}\, u_\mathrm{f})/\partial\tau = 0$, additional assumptions are introduced, i.e. for $h_\mathrm{f}$,

$$\frac{\mathrm{d}h_\mathrm{f}}{\mathrm{d}s} = c_\mathrm{p}\left(\frac{\mathrm{d}T_\mathrm{f}}{\mathrm{d}s}\right) \tag{19}$$

and $d_\mathrm{f}$ and $\dot{V}_\mathrm{f}$ are constant. Using all these simplifications we obtain

$$\frac{\mathrm{d}T_\mathrm{f}}{\mathrm{d}s} = \frac{2\pi r(s)i(s)E}{d_\mathrm{f}c_\mathrm{p}\dot{V}_\mathrm{f}} \tag{20}$$

The equation of motion is based on a momentum balance. The balance applies to both phases and plug flow is also assumed for both phases.

$$\frac{\partial}{\partial\tau}(d_\mathrm{g}A_\mathrm{g}v_\mathrm{g} + d_\mathrm{f}A_\mathrm{f}v_\mathrm{f}) = -\frac{\partial}{\partial_\mathrm{s}}(d_\mathrm{g}A_\mathrm{g}v_\mathrm{g}^2 + d_\mathrm{f}A_\mathrm{f}v_\mathrm{f}^2) - A\left(\frac{\partial p}{\partial s}\right) - (\tau_\mathrm{A} + \tau_\mathrm{C})\, 2\pi r(s) \tag{21}$$

where $\tau_\mathrm{A}$ and $\tau_\mathrm{C}$ are the shear stresses acting on the anode and the cathode surfaces. The term with the shear stresses may be approximated by the equation valid for parallel plates,

$$(\tau_\mathrm{A} + \tau_\mathrm{C})\, 2\pi r(s) = \left(\frac{K}{Re_\mathrm{M}^\mathrm{n}}\right)\left(\frac{1}{D_\mathrm{ekv}}\right)\left[\left(\frac{1}{2}\right)d_\mathrm{f}\right]\left[\frac{\dot{V}_\mathrm{f}^2}{A(1-\alpha)}\right] \tag{22}$$

where $D_\mathrm{ekv} \approx 2g(s)$, and $Re_\mathrm{M} < 2300$, $K = 96$, $n = 1$ in the laminar region and $Re_\mathrm{M} > 2300$, $K = 0.316$, $n = 0.25$ for the turbulent region.

$$Re_\mathrm{M} = \left(\frac{\dot{V}_\mathrm{f}}{A}\right)\left(\frac{D_\mathrm{ekv}}{v_\mathrm{f}}\right)(1-\alpha)^{2.5} \tag{23}$$

The correction term $(1 - \alpha)^{2.5}$ in Equation 23 was introduced by Brinkman [6] and Roscoe [7] for suspension formed by solid spheres. It is known that gas bubbles behave like solid spheres in the presence of surface active agents in the electrolyte.

Further, the following term may be rearranged

$$d_\mathrm{g}A_\mathrm{g}v_\mathrm{g}^2 + d_\mathrm{f}A_\mathrm{f}v_\mathrm{f}^2 = [d_\mathrm{g}\dot{V}_\mathrm{g}^2 + (d_\mathrm{g} + d_\mathrm{f})\dot{V}_\mathrm{f}\dot{V}_\mathrm{g} + d_\mathrm{f}\dot{V}_\mathrm{f}^2]/A \tag{24}$$

For the steady state, $\partial(d_\mathrm{g}A_\mathrm{g}v_\mathrm{g} + d_\mathrm{f}A_\mathrm{f}v_\mathrm{f})/\partial\tau = 0$, we obtain from Equation 21,

$$\frac{\mathrm{d}p}{\mathrm{d}s} = -\left(\frac{1}{A}\right)\left(\frac{\mathrm{d}}{\mathrm{d}s}\right)[(d_\mathrm{g}\dot{V}_\mathrm{g}^2 + d_\mathrm{g}\dot{V}_\mathrm{f}\dot{V}_\mathrm{g} + d_\mathrm{f}V_\mathrm{f}^2 + d_\mathrm{f}\dot{V}_\mathrm{f}\dot{V}_\mathrm{g})/A] - (\tau_\mathrm{A} + \tau_\mathrm{C})\, 2\tau r(s)/A \tag{25}$$

or using Equations 14 to 17 we have

$$\frac{dp}{ds} = -\left\{\frac{1}{A^2}\left\{2\dot{V}_g\left[\frac{d(d_g\dot{V}_g)}{ds}\right] - \dot{V}_g^2\left[\left(\frac{1}{p}\right)d_g\left(\frac{dp}{ds}\right) - \left(\frac{1}{T}\right)d_g\left(\frac{dT}{ds}\right)\right] + \dot{V}_f\left[\frac{d(d_g\dot{V}_g)}{ds}\right]\right.$$
$$+ d_g\dot{V}_g\left(\frac{d\dot{V}_f}{ds}\right) + d_f\dot{V}_g\left(\frac{d\dot{V}_f}{ds}\right) + \frac{d_f\dot{V}_f}{d_g}\left[\frac{d(\dot{V}_g d_g)}{ds}\right] - \frac{d_f\dot{V}_g\dot{V}_f}{d_g}\left[\left(\frac{1}{p}\right)d_g\left(\frac{dp}{ds}\right) - \left(\frac{1}{T}\right)d_g\left(\frac{dT}{ds}\right)\right]$$
$$\left. + d_f 2\dot{V}_f\left(\frac{d\dot{V}_f}{ds}\right)\right\} - \frac{1}{A^3}[2\pi g(s) + 2\pi r(s)]\left(\frac{dg(s)}{ds}\right)(d_g\dot{V}_g^2 + d_g\dot{V}_f\dot{V}_g + d_f\dot{V}_f^2 + d_f\dot{V}_f\dot{V}_g)\Big\}$$
$$- (\tau_A + \tau_C)\,2\pi r(s)/A \tag{26}$$

After elimination of pressure derivatives, the right hand side of Equation 19c contains only known derivatives.

Eliminating all derivatives of pressure, we obtain a multiplier of $dp/ds$ denoted as $f$.

$$f = 1 - d_g\dot{V}_g^2\left(\frac{1}{pA^2}\right) - d_f\dot{V}_f\dot{V}_g\left(\frac{1}{pA^2}\right) \tag{27}$$

Usually $f > 0$, but if $f \leqslant 0$ (in some cases), then the pressure loss should increase to infinity; this represents the condition of choking for the ECM process. The choking condition expressed by Equation 27 may be transformed to a more convenient form by introducing density ratio, $d_R$, and Euler number, $Eu$:

$$d_R = \frac{d_f}{d_g} \tag{28}$$

$$Eu = \frac{p}{d_f(\dot{V}_f/A)^2} \tag{29}$$

$$\frac{\dot{V}_g}{\dot{V}_f} \leqslant -\frac{d_R}{2} + \left[Eud_R + \left(\frac{d_R}{2}\right)^2\right]^{1/2} \tag{30a}$$

If $\dot{V}_g/\dot{V}_f$ in a given system is lower than the right hand side of Equation 30a, then the choking condition is not fulfilled and ECM proceeds without operating problems.

Another possibility for expressing Equation 30a is

$$\frac{d_g\dot{V}_g}{d_f\dot{V}_f} \leqslant -\frac{1}{2} + \left[\frac{Eu}{d_R} + \frac{1}{4}\right]^{1/2} \tag{30b}$$

or

$$\alpha \leqslant \left\{-\frac{d_R}{2} + \left[Eud_R + \left(\frac{d_R}{2}\right)^2\right]^{1/2}\right\}\Big/\left\{1 - \frac{d_R}{2} + \left[Eud_R + \left(\frac{d_R}{2}\right)^2\right]^{1/2}\right\} \tag{30c}$$

## 3. Discussion

### 3.1. *Choking condition*

In some industrial processes the inlet electrolyte is mixed with air or carbon dioxide. The inlet void fraction is $\alpha \in \langle 0.2; 0.7\rangle$ and the inlet pressure $p \in \langle 0.5; 2.0\rangle$ MPa, $T \approx 300$ K, $d_f \approx 1000\,\mathrm{kg\,m^{-3}}$. The value of $M_{g,c}$ for air is $28.8 \times 10^{-3}\,\mathrm{kg\,mol^{-1}}$ and for $CO_2$ is $44 \times 10^{-3}\,\mathrm{kg\,mol^{-1}}$.

Let us denote the right hand side of Equation 30c as $\alpha_M$. Fig. 2 shows $\alpha_M$ versus $p$ with $\dot{V}_f/A$, the superficial electrolyte velocity, as parameter. Let us discuss the process of ECM starting with

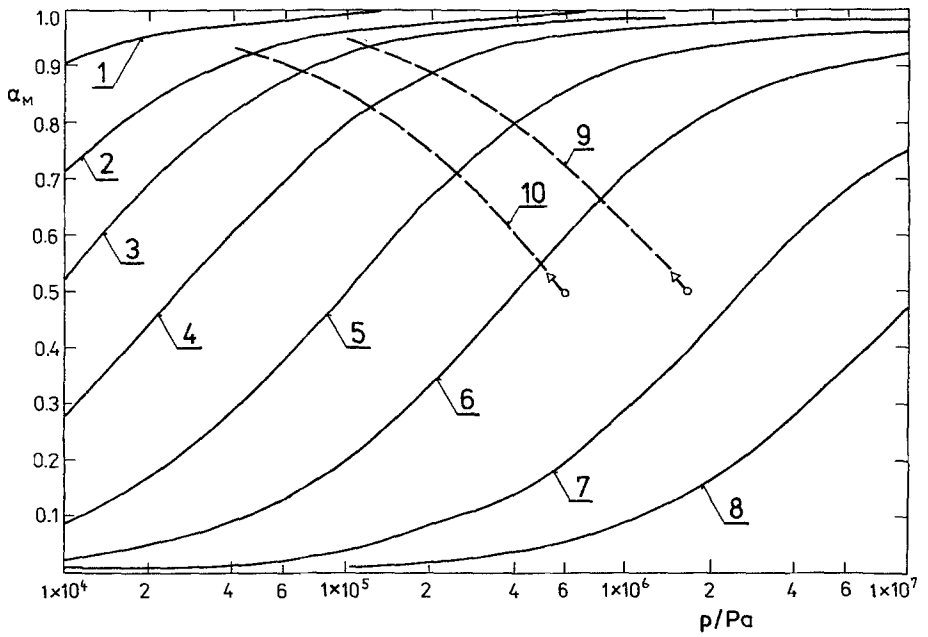


Fig. 2. Void fraction of gas versus static pressure for different superficial velocities of electrolyte according to Equation 30c; $d_f = 10^3\,\mathrm{kg\,m^{-3}}$, $M_g = 28.8 \times 10^{-3}\,\mathrm{kg\,mol^{-1}}$ (air). Solid lines give values of $\dot{V}_f/A$; (1) $1\,\mathrm{m\,s^{-1}}$; (2) $2\,\mathrm{m\,s^{-1}}$; (3) $3\,\mathrm{m\,s^{-1}}$; (4) $5\,\mathrm{m\,s^{-1}}$; (5) $10\,\mathrm{m\,s^{-1}}$; (6) $20\,\mathrm{m\,s^{-1}}$; (7) $50\,\mathrm{m\,s^{-1}}$; (8) $100\,\mathrm{m\,s^{-1}}$. Dashed lines give expansion of the air–electrolyte mixture, where $\alpha_0 = 0.5$, for the following values of the static pressure at the inlet (9) 1.6 MPa; (10) 0.6 MPa.

a mixture of gas and electrolyte, $\dot{V}_g = \dot{V}_f = 1 (\alpha_0 = 0.5)$, at an inlet pressure of 1.6 MPa (see Fig. 2, curve 9). We assume that the increase of $V_g$ due to electrolysis is negligible along the gap. The interelectrode gap can be approximated by a rectangular channel, so that the $\dot{V}_f/A$ value along the gap is constant. If the pressure loss along the gap exceeds 1.0 MPa, then for $\dot{V}_f/A = 20\,\mathrm{m\,s^{-1}}$ the static exit pressure is less than (1.6 MPa − 1.0 MPa) ⩽ 0.6 MPa, and from curve 9 of Fig. 2 we see that the choking condition is fulfilled ($\alpha_e > \alpha_M$).

Working only with $10\,\mathrm{m\,s^{-1}}$ for $\dot{V}_f/A$ and with the same pressure loss 1.0 MPa, the exit pressure of 0.6 MPa guarantees that choking cannot start ($\alpha_M > \alpha_e$). To ensure a high static pressure at the exit of the gap, it is necessary to use a flow restrictor dam in the exit [4].

From Fig. 2 we can also see the limits for $\alpha$ values at the exit part of the gap for different $\dot{V}_f/A$ values. For $\dot{V}_f/A = 20\,\mathrm{m\,s^{-1}}$ and $p_e = 0.1$ MPa the $\alpha_e$ value should be lower than 0.19, otherwise choking will occur.

### 3.2. *Comparison with published results [5]*

The choking limits given by Equation 78 in [5] are only a crude approximation of Equations 27 and 30. The main reason is a drastic simplification of the momentum balance as represented by Equation 44 in [5].

The choke limits for flat and spherical tools are given in [5] for different exit pressures, most of them for $p_e = 0.206$ MPa. For other parameters given in Table 1 this exit pressure for flat radial tools could be reached only at a very small feed rate ($f_r \leqslant 1 \times 10^{-5}\,\mathrm{m\,s^{-1}}$). At higher feed rates of the tool the pressure at the exit of the gap should always be higher than 0.2 MPa, even for $p_0 = 0.01$ MPa, because the radial tool acts as a radial diffuser [8–15] and the static pressure at the exit, for the given conditions, is higher than 0.2 MPa (see Fig. 3). This is the main reason why the results presented in graphical form in [5] are not valid for parameters given in Table 1 if the inlet is situated in the centre of the tool.

*Table 1. List of input parameters used for all calculations*

| *Parameter* | *Value* |
|---|---|
| $c_p$ | $2.9076 \times 10^3\ \mathrm{J\,kg^{-1}\,K^{-1}}$ |
| $D$ | 0.03175 m |
| $d$ | 0.0635 m |
| $d_m$ | $7801.1\ \mathrm{kg\,m^{-3}}$ |
| $d_f$ | $993.16\ \mathrm{kg\,m^{-3}}$ |
| $E$ | 16 V |
| $\varrho_{f,0}$ | 0.03598 Ωm |
| $p_0$ | 0.01 MPa or 0.2068 MPa |
| $R_g$ | $8.314\ \mathrm{J\,K^{-1}\,mol^{-1}}$ |
| $T_0$ | 298 K |
| $\gamma_R$ | $-0.00888\ \mathrm{K^{-1}}$ |
| $\varepsilon_a$ | $2.889 \times 10^{-7}\ \mathrm{kg\,A^{-1}\,s^{-1}}$ (Fe) |
| $\varepsilon_g$ | $1.032 \times 10^{-8}\ \mathrm{kg\,A^{-1}\,s^{-1}}$ ($H_2$) |
| $\nu_f$ | $6.9677 \times 10^{-7}\ \mathrm{m^2\,s^{-1}}$ |
| $\sigma$ | 1 |
| $\dot{V}_{f,o}$ | $6.3 \times 10^{-4}\ \mathrm{m^3\,s^{-1}}$ |
| $f_r$ | $\in \langle 5 \times 10^{-6};\ 8 \times 10^{-5} \rangle\ \mathrm{m\,s^{-1}}$ |
| $\cos \Theta(s)$ | 1 |

Figs 3–7 were obtained by numerical solution of Equation 26 (after a rearrangement), together with Equations 14b, 16, 17b and 20, and using Equation 10b, 11, 12 and 15.

The dimension of the inlet gap as a function of the feed rate of the cathode is plotted in Fig. 4. The superficial velocity of the electrolyte ($\dot{V}_f/A$) at the inlet and exit of the gap is a linear function of the feed rate (see Fig. 5). The exit void fraction of gas versus the feed rate may be seen from Fig. 6. The decrease of $\alpha_e$ with increasing feed is given by the increase of the exit pressure (see Fig. 3).

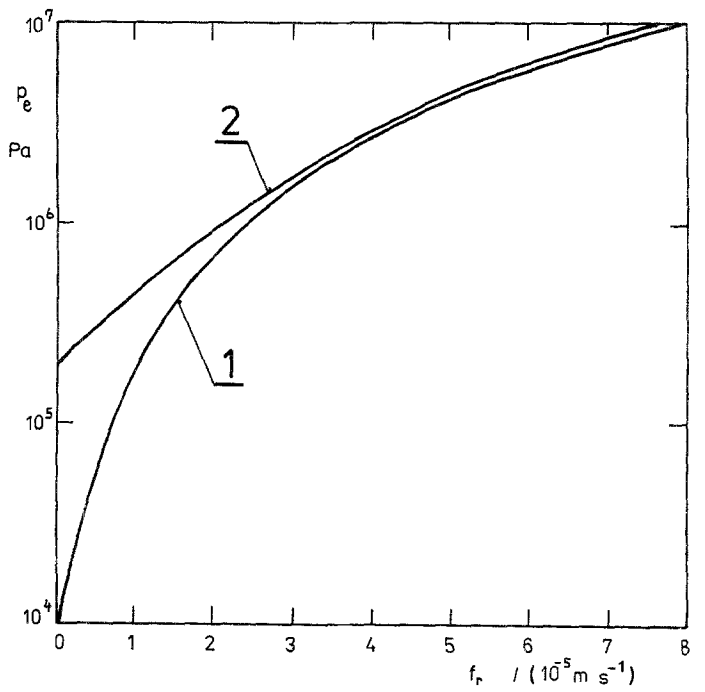


Fig. 3. Exit pressure versus feed rate of the flat tool for conditions given in Table 1. Values of inlet pressure: (1) 0.01 MPa; (2) 0.207 MPa.

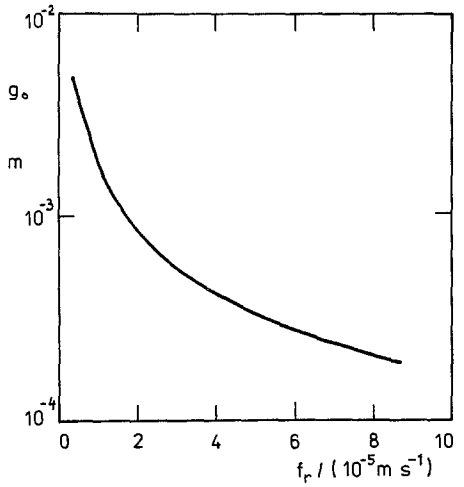


Fig. 4. Inlet gap versus feed rate of the flat tool for conditions given in Table 1. Input pressure, 0.01 MPa.

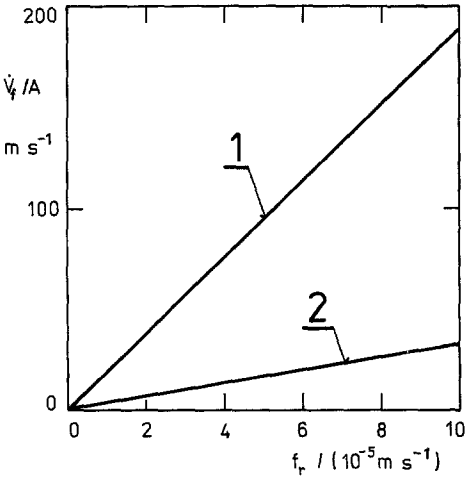


Fig. 5. Superficial velocity of the electrolyte versus feed rate of the cathode: (1) at the inlet of the gap; (2) at th exit of the gap. Other conditions given in Table 1.

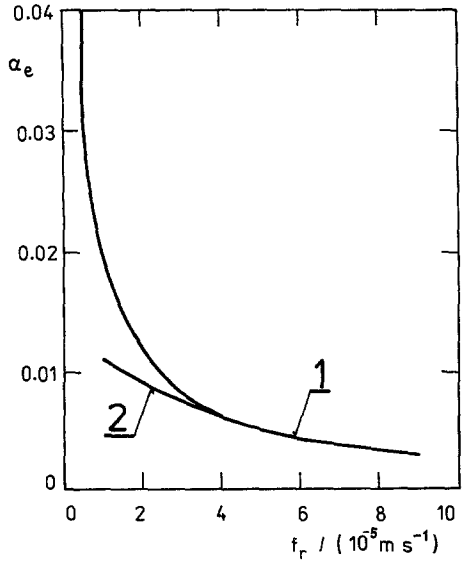


Fig. 6. Exit void fraction of gas versus feed rate of the cathode for conditions given in Table 1. Values of inlet pressure: (1) 0.01 MPa; (2) 0.207 MPa.

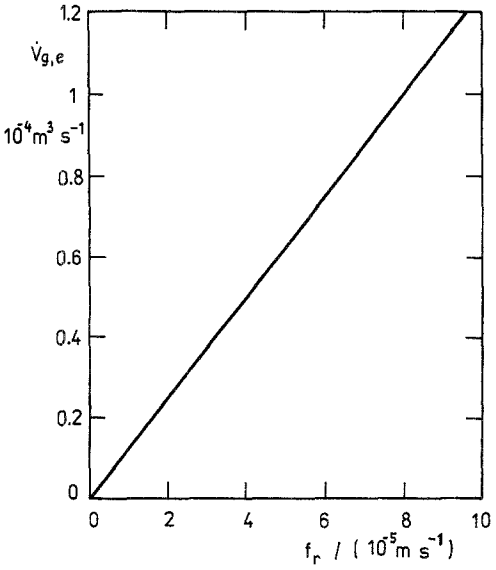


Fig. 7. Exit volumetric flow rate of the gas, recalculated for pressure 0.2 MPa, versus feed rate of the flat tool. Other conditions given in Table 1.

Due to the high pressure at the inlet ($p_0 > 10^4$ Pa), no choking was observed at the feed rates $f_r \geqslant 5 \times 10^{-6}\,m\,s^{-1}$ (see Figs 3–6). This result is in good agreement with the values in Fig. 2.

If the inlet of the electrolyte is located on the outer radius of the tool ($D$) and the flow is directed to the centre of the tool, the situation is rather different. The inlet pressures are very close to the $p_e$ values in Fig. 3, and the outlet values of the pressure may reach 0.2 MPa. The approximate void fraction can then be calculated using the values of $\dot{V}_g$ from Fig. 7.

(i) For $f_r = 8 \times 10^{-5}\,m\,s^{-1}$. The inlet pressure is $\sim 11$ MPa, the inlet superficial velocity of electrolyte is only $\sim 26\,m\,s^{-1}$, the exit pressure is 0.2 MPa, the outlet superficial velocity is $\sim 150\,m\,s^{-1}$. From Fig. 7, $\dot{V}_{g,e}$ equals $1 \times 10^{-4}\,m^3\,s^{-1}$ and from Table 1, $\dot{V}_{f,o} = 6.3 \times 10^{-4}\,m^3\,s^{-1}$. The exit void fraction is $\alpha_e = 0.137$. For $\dot{V}_f/A = 150\,m\,s^{-1}$, $\alpha_M$ is $\approx 0.02$ (see Fig. 2). This means that for the flow in the gap the choking condition is fulfilled; $\alpha_e > \alpha_M$.

(ii) For $f_r = 2 \times 10^{-5}\,m\,s^{-1}$. The inlet pressure is $\sim 1$ MPa, the inlet superficial velocity $\sim 6\,m\,s^{-1}$, the exit pressure is 0.2 MPa, the outlet superficial velocity $\sim 38\,m\,s^{-1}$, $\dot{V}_{g,e} \sim 0.25 \times 10^{-4}\,m^3\,s^{-1}$, $\alpha_e = 0.038$. However, for $\dot{V}_f/A = 38\,m\,s^{-1}$ and $p_e = 0.206$ MPa, $\alpha_M$ is $\sim 0.12$.

This means that $\alpha_M > \alpha_e$ and in this case no choking is expected. From the calculated examples it follows that at $f_r > \sim 3$–$4 \times 10^{-5}\,m\,s^{-1}$ the choking condition is always met.

## 4. Conclusion

Equations 27 and 30 allow calculation of the limiting void fraction, $\alpha_M$, required for the generation of choking, as a function of the following operating parameters: static pressure, superficial electrolyte velocity, temperature, electrolyte density and density of the gas. The use of Equations 27 and 30 is restricted to uni-directional flows in channels and flat or shallow axially symmetric cavities with radial inflow and outflow. The possibility of using the inlet mixture of gas and electrolyte can easily be discussed using Fig. 2. The use of flat and spherical tools at inlet pressures higher than 0.01 MPa, values of $\dot{V}_f/A$ over a broad range of 10–150 $m\,s^{-1}$ and for $f_r > 5 \times 10^{-6}\,m\,s^{-1}$, $d \sim 0.006$ m and $D \sim 0.03$ m, proceeds without choking for a radial inflow located in the centre of the tool.

For a flat radial tool with electrolyte inlet located on the outer diameter and the electrolyte flow directed to the centre of the tool, the choking condition is fulfilled for $f_r > (3$–$4) \times 10^{-5}\,m\,s^{-1}$ and $p_e = 0.206$ MPa. Other parameters important for ECM can be found in Table 1. For $f_r < \sim 3 \times 10^{-5}\,m\,s^{-1}$, choking is not possible for the system under consideration.

## References


[1] J. A. McGeough, 'Principles of Electrochemical Machining', Chapman and Hall, London (1974) p. 141.
[2] W. G. Clark and J. A. MaGeough, Paper presented at First Int. Conf. on ECM, Leicester University, March 1973.
[3] J. F. Thorpe and R. D. Zerkle, *Int. J. Mach. Tool Des. Res.* **9** (1969) 131.
[4] J. F. Wilson, 'Practice and Theory of Electrochemical Machining', Wiley Interscience, New York (1971) p. 126.
[5] J. F. Thorpe and R. D. Zerkle, in 'Fundamentals of ECM' (edited by C. L. Faust), Electrochemical Society, Princeton (1961) p. 1.
[6] H. C. Brinkman, *J. Chem. Phys.* **20** (1952) 571.
[7] R. Roscoe, *Brit. J. Appl. Phys.* **3** (1952) 267.
[8] P. S. Moller, *Aeronaut. Q.* **14** (1963) 163.
[9] *Idem, J. Basic Engng Trans. ASM* **88** (1966) 155.
[10] T. Kawaguchi, *Bull. JSME* **14** No. 70 (1971) 355.
[11] I. L. Parmet and E. Saibel, *Rev., Roum. Sci. Techn., Mech. Appl.* **11** (1966) 275.
[12] J. C. Patrat: *J. Mécanique* **14** (1975) 505.
[13] J. L. Peube, *ibid.* **2** (1963) 377.
[14] Chen, Che-Pen, *ibid.* **5** (1966) 245.
[15] M. S. Kdader and R. I. Vachon, *Int. J. Mech. Sci.* **15** (1973) 221.